Collective Bosonic Excitations in Doped para-H2 Clusters through the Full Configuration Nuclear Orbiatl Approach

ARTICLE *in* JOURNAL OF PHYSICAL CHEMISTRY LETTERS · SEPTEMBER 2011

Impact Factor: 7.46 · DOI: 10.1021/jz200801r

1 AUTHOR:

Maria Pilar De Lara-Castells
Spanish National Research Council
72 PUBLICATIONS **726** CITATIONS

THE JOURNAL OF PHYSICAL CHEMISTRY Letters

LETTER

pubs.acs.org/JPCL

Collective Bosonic Excitations in Doped *para*-H_2 Clusters through the Full-Configuration-Interaction Nuclear Orbital Approach

María Pilar de Lara-Castells*,† and Alexander O. Mitrushchenkov‡,§

†Instituto de Física Fundamental (C.S.I.C.), Serrano 123, E-28006, Madrid, Spain

‡Université Paris-Est, Laboratoire Modélisation et Simulation Multi Echelle, MSME UMR 8208 CNRS, 5 bd Descartes, 77454 Marne-la-Vallée, France

Supporting Information

ABSTRACT: The onset of collective rotational states as minima in the energy spectra of bosonic spinless *para*-H_2 (pH_2) molecules confined in a belt around a molecular dopant is studied by analyzing excites states in $(pH_2)_N$-CO_2 clusters ($N \leq 5$). These minima result from a combined effect of a bosonic-symmetry-induced boundary periodic condition in cyclic arrangements of pH_2 and the increasingly intensified hard-core of the effective pH_2-pH_2 interaction as N increases. The same also applies to doped ^{4}He clusters in a contrast with the fermionic ^{3}He case ($N \leq 4$). The onset of the minima for pH_2 and ^{4}He marks a reversal in the apparent scaling of the rotational constant with N for the axial rotation around the dopant (from inversely proportional to proportional), whereas the ^{3}He counterpart retains the regular dependence. The newly developed full-configuration-interaction nuclear orbital approach for bosons is presented here for the first time.

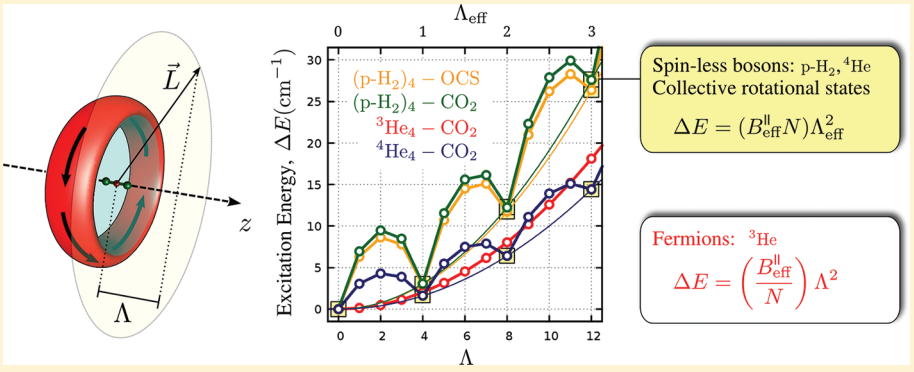

SECTION: Molecular Structure, Quantum Chemistry, General Theory

Low-temperature spectroscopy of molecules in highly quantal fluids has provided important information on interesting properties of the environment such as ^{4}He (^{3}He) superfluid (normal fluid) effects[1] and demonstrated the key role of bosonic (fermionic) nuclear statistical effects. Because a *para*-H_2 (pH_2) molecule has a total nuclear spin equal to zero and at low temperatures only the lowest $J = 0$ state is populated, it can be considered to be a spinless boson, similar to ^{4}He, but twice as light. Hence, a doped pH_2 cluster might be expected to behave similarly to the ^{4}He counterpart, including the onset of superfluidity as predicted by Sindzingre et al.[2] for pure pH_2 clusters. and motivating experimental[3] and theoretical[4] studies. However, the three times deeper attractive well of the pH_2-pH_2 potential as compared with the ^{4}He case causes the solidification of bulk pH_2 at relatively low temperatures ($T_c \approx 14$ K). This makes doped pH_2 clusters a good model to address more general issues such as the possible existence of a supersolid phase.[5,6] Therefore, experimental and theoretical[7,8] spectroscopic studies of molecular dopants in $(pH_2)_N$ clusters, both in gas phase and inside helium nanodroplets, have been carried out during the past few years (see, e.g., ref 9 and references therein). One intriguing experimental result interpreted in terms of microscopic superfluidity is the disappearance of the Q branch in the rovibrational infrared spectra of linear host molecules such as carbonyl sulfide (OCS) for just five and six pH_2 molecules on a belt encircling the dopant with the OCS-$(pH_2)_N$ complex coated by a helium nanodrop.[10] The presence of molecular superfluidity has also been shown via a nonclassical evolution of the dopant rotational constant with cluster size in a very recent combined experimental/theoretical study of gas-phase CO_2-$(pH_2)_N$ ($N \leq 18$) clusters by Li et al.[11] From finite-temperature path-integral Monte Carlo (PIMC) simulations, the superfluid fraction along the axis perpendicular to the dopant was determined and used to aid the experimental estimations.[11]

Despite important recent progress, detailed studies of excited and disentangled states in doped $(pH_2)_N$ are still lacking and recently a renewed interest has arisen concerning them.[9] As compared with the highest symmetry and nodeless wave function of bosons in the ground state, excited states are more difficult to address with quantum Monte Carlo treatments because of the wave function sign problem.[12] Alternatively, we have extended and further optimized the full-configuration-interaction nuclear-orbital (FCI-NO) method, previously developed and applied to doped ^{3}He clusters[13−17] to the bosonic case. The treatment

Received: June 14, 2011
Accepted: August 4, 2011
Published: August 04, 2011

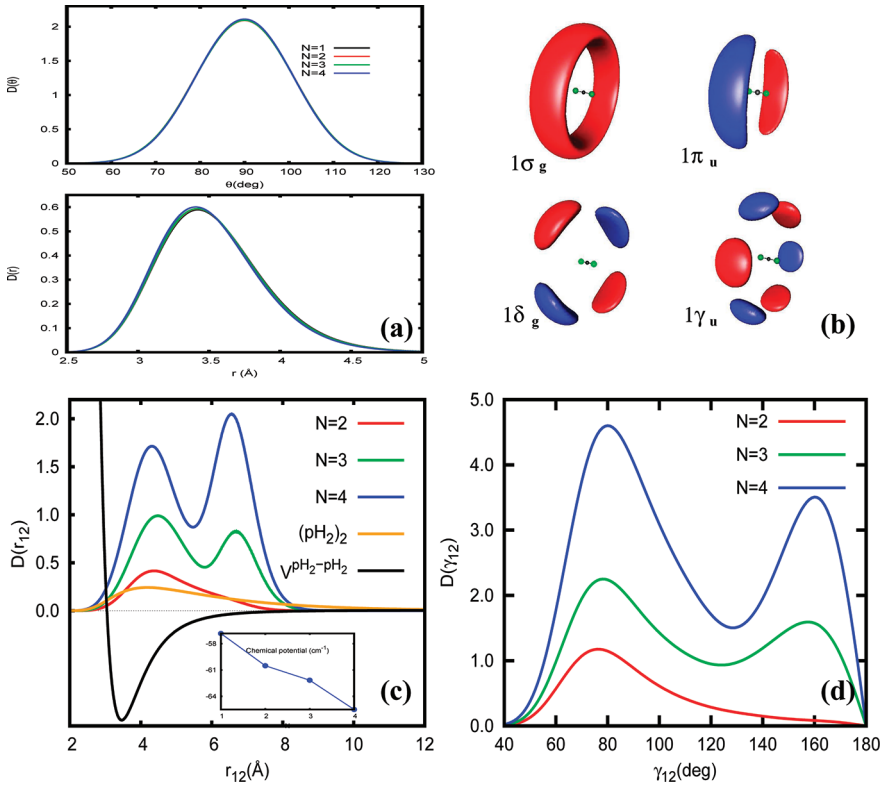

Figure 1. $(pH_2)_N$-CO_2 clusters ($N \leq 4$): (a) angular (upper panel) and radial (lower panel) one-particle density distributions; (b) isoprobability surfaces for the natural orbitals ($N = 4$), where the blue and red colors indicate positive and negative lobes; (c) radial pair density distributions and chemical potential (inset); and (d) angular pair density distribution where γ_{12} is defined as the angle between the position vectors of two bosons, $\cos \gamma_{12} = \mathbf{r}_1 \cdot \mathbf{r}_2 / r_1 r_2$.

relies on the so-called quantum-chemistry-like (QC) approach, first proposed by Jungwirth and Krylov,[18] which considers the solvent species as "pseudo-electrons" and the atoms composing the dopant molecule as "pseudo-nuclei", replacing electron−electron and electron−nucleus Coulomb interactions by the solvent−solvent and the solvent−dopant pair potentials. This way, all nuclear-statistic-induced (bosonic or fermionic) symmetry effects are automatically included and ground- and excited-state wave functions can be calculated with similar accuracy. Major difficulties preventing free-parameter implementations are caused by the highly repulsive potential between the coating species (the so-called hard-core problem). Within the FCI-NO treatment, this problem was successfully solved by replacing the commonly used Davidson algorithm of diagonalization by a Jacobi−Davidson solver.[13,14] A QC-like ansatz was also used in Hartree/Hartree−Fock implementations with a softened repulsive core (see, e.g., ref 19 and references therein). Closely related CI treatments for $J = 0$ cluster states were developed by Villarreal et al.[20] and Hernández et al.[21] with $N = 2$ and Felker[22] with $N \leq 5$.

Within the FCI-NO approach and using Fock space notations to label uniquely the configuration state functions (CSFs) of N spinless (e.g., pH_2) bosons, $|I\rangle = |n_1 n_2 ... n_M\rangle$, where M is the number of orbitals and n_i is the occupation number of the ith orbital ($N = \sum_i n_i$). The Hamiltonian of the pair-interacting bosonic system confined by the external boson-dopant potential v_{ext} is given by

$$\hat{H} = \sum_{ij} h_{ij} b_i^\dagger b_j + \frac{1}{2} \sum_{ijkl} V_{ijkl} b_i^\dagger b_k^\dagger b_l b_j$$

where h_{ij} and V_{ijkl} are the one- and two-particle integrals. Considering the molecular dopant as fixed and using satellite coordinates $\mathbf{r}_i$ to define the position of the ith boson with respect to the dopant mass center, the one-particle operator $\hat{h}(\mathbf{r})$ reads

$$\hat{h}(\mathbf{r}) = -\frac{\hbar^2}{2\mu} \frac{\partial^2}{\partial r^2} + \frac{\mathbf{l}^2}{2\mu r^2} + v_{ext}(r, \theta) \qquad (1)$$

with μ and $\mathbf{l}$ being the boson-dopant reduced mass and the angular momentum associated with $\mathbf{r}$, respectively. (θ is the angle between the dopant axis and $\mathbf{r}$.) The two-particle operator is simply the pairwise interaction potential between the bosonic species, $V(r_{12})$. The creation/annihilation actions of the operators on a given CSF are $b_i |n_1 n_2 ... n_i ... n_M\rangle = (n_i)^{1/2} |n_1 n_2 ... n_i - 1 ... n_M\rangle$ and $b_i^\dagger |n_1 n_2 ... n_i ... n_M\rangle = (n_i + 1)^{1/2} |n_1 n_2 ... n_i + 1 ... n_M\rangle$. By using these expressions, algorithms similar to the fermionic case[13] have been implemented to evaluate one- and two-particle matrix elements with the one-particle basis set comprising spherical harmonics $Y_{lm}(\theta,\phi)$ and numerical radial functions $F_n(r)$ (see, e.g., refs 19 and 20). Moreover, a new implementation of the FCI-NO method that uses an optimized basis set for highly anisotropic boson-dopant interactions has been developed; see below.

As an illustrative example, we consider carbon dioxide as the molecular impurity with effective one- and two-dimensional pH_2−pH_2 and pH_2−CO_2(000) potentials from ref 23. One-particle and pair densities along with isoprobability surfaces for the most relevant natural orbitals of ground-state $(pH_2)_N$-CO_2 complexes ($N \leq 4$) are displayed in Figure 1. Owing to the strong anisotropy of the dopant-pH_2 PES with a minimum at a

dx.doi.org/10.1021/jz200801r | J. Phys. Chem. Lett. 2011, 2, 2145–2151

T-shaped geometry, the angular density distributions are clearly peaked at $\theta = 90°$, whereas the peak position of the radial density distribution r_{eq} is at 3.4 Å. As apparent from Figure 1, both distributions depart very little from the independent-particle (IP) case, and, as a result, the averaged $\langle v_{ext} \rangle$ values fit to better than 1% N times that of the IP case. The relevant natural orbitals (Figure 1b) are thus all located on a centered belt around the internuclear axis. Starting with the belt-like $1\sigma_g$ orbital, the close-lying excited $1\pi_u$ orbital describes quantized rotations on the belt (1-D rigid rotor states) with an excitation energy approximately given by $B^{\parallel}_{eff} \times l_z^2$, where $B^{\parallel}_{eff}$ is an effective rotational constant for the axial rotation around the CO_2 axis. It is equal to the average $\langle (1/2)\mu r^2 \rangle$ for the $1\sigma_g$ state, and l_z is the $\mathbf{l}$ projection on the CO_2 axis. Despite the high fractional occupation numbers of the natural orbitals, four of them are enough to account for >93% of the pH_2 population. The largest coefficient of the FCI wave function comes from the $(1\sigma_g)^N$ configuration with an absolute value decreasing as N increases. Because of the hard-core and the well-depth of the pH_2-pH_2 potential,[15] the pH_2 molecules are promoted to excited IP rotational states. This is reflected by the averaged kinetic energy, which is higher than that of N ground-state pH_2-dopant dimers by up to 16%. The relative location of the pH_2 molecules on the belt is clarified by the radial and angular pair density distributions $D(r_{12})$ and $D(\gamma_{12})$ (see lower panels in Figure 1). For $N = 2$, the $(pH_2)_2$ pair locates at one side of the belt, encircling the dopant and $D(\gamma_{12})$ [$D(r_{12})$] peaks at $\gamma_{12} \approx 80°$ ($r_{12} \approx 2 \times r_{eq} \times \sin(\gamma_{12}/2) =$ 4.4 Å). This is in line with a very recent study of the CO_2-$(pH_2)_2$ cluster.[24] For $N = 3$, a second peak appears at $\gamma_{12} \approx 160°$, and the second maximum in $D(r_{12})$ locates at 6.6 Å (i.e., close to $2 \times r_{eq} \times \sin(\gamma_{12}/2) = 6.7$ Å). The pH_2 trimer is arranged in an isosceles triangular structure in which two pH_2 partners remain too far away to benefit from the minimum. As a result, the averaged two-particle potential energy (-15.2 cm^{-1}) is almost twice the value attained for $N = 2$. For $N = 4$, the average $\langle V^{pH_2-pH_2} \rangle$ is about -30.0 cm^{-1}, only -0.4 cm^{-1} below four times the value for a $(pH_2)_2$ pair (about -7.6 cm^{-1}). The results indicate a cyclic arrangement of the $(pH_2)_4$ tetramer around the dopant's mass center. Notice that the most probable structure is not the classical one of four pH_2 molecules equally spaced on the belt plane. As in previous studies,[25,26] this almost ideal structure is reached at completion on the belt with five pH_2 molecules. We notice that the peak positions of the $D(r_{12})$ distributions (around 4.4 and 6.6 Å) are very close to the values attained in pure $(pH_2)_N$ clusters (~4.2, as shown in Figure 1a for $(pH_2)_2$, and 6.8 Å in ref 9).

Our results for the ground state are consistent with previous findings through DMC[26,27] and PIMC calculations[11] with OCS and CO_2 as the dopant molecules. The one-particle densities for the low-lying excited states are nearly coincident with those of the ground state, which means that the pH_2 molecules still locate on the centered belt around the dopant axis. These excited states can be labeled by Λ, the projection of the total angular momentum $\mathbf{L} = \Sigma_i^N \mathbf{l}_i$ on the dopant axis, which is a good quantum number. Focusing on the first excited state, two trends should be stressed (see Table 1): (1) From $N = 2$ onward, the larger the number of pH_2 species, the higher the promotion energy to the first excited state. (2) From $N = 4$ onward, the Λ value for the first excited state equals the number of pH_2 molecules N, the ground and the first excited states share almost identical pair density distribution, and the excitation energy is about $NB^{\parallel}_{eff}$. Similar trends hold for doped ^{4}He clusters in contrast with the fermionic ^{3}He case (see below) and also considering OCS as the dopant molecule; see the Supporting Information. We notice that the dopant has been treated as a nonrotating molecule, omitting the Coriolis couplings between Λ and $\Lambda \pm 1$ states. The relative small values found for the Coriolis couplings in preliminary calculations (<10% of the total angular momentum average) and the large energy difference between the states that can be coupled by these terms (>20 cm^{-1} considering pH_2 and CO_2) show the validity of the approach of decoupling the quantum-solvent motion from the dopant rotation.

Table 1. Total Energies (inverse centimeters) and Associated Λ Values of the Four Lowest-Energy States for $N = 1-5$ using the $Y_{lm}(\theta,\phi)R_n(R)$ ($l_{max} = m_{max} = 9$, $n = 4$) and the $(0,0)e^{-im\phi}$ ($50 \le m_{max} \le 120$) Basis Sets

Λ	$N = 1$	$N = 2$	$N = 3$	$N = 4$	$N = 5$
			$Y_{lm}(\theta,\phi)R_n(R)$ One-Particle Basis Set		
0	−56.84	−117.34	−179.50	−245.01	
1	−56.48	−117.16	−178.32	−236.27	
2	−53.74	−116.46	−177.16		
3	−50.38	−113.86	−177.35		
4				−241.33	
			$(0,0)e^{-im\phi}$ One-Particle Basis Set		
0	−57.66	−118.60	−181.36	−247.80	−308.23
1	−56.90	−118.07	−180.08	−240.82	−284.54
2	−54.63	−117.08	−179.32	−238.30	
3	−50.85	−115.06	−179.10		
4				−244.73	−282.27
5					−304.45

With the basis set comprising spherical harmonics (400 orbitals), FCI calculations for more than four bosons are unfeasible. A new implementation that uses 2-D (r,θ) orbitals and complex exponentials for the azimuthal degree of freedom $e^{-im\phi}/(2\pi)^{1/2}$ has been developed. These (r,θ) orbitals are obtained by numerically solving the one-particle Schrödinger equation as will be reported elsewhere. By denoting the lowest-energy orbital as (0,0), which is similar to the belt-like $1\sigma_g$ orbital displayed in Figure 1b, the wave function of ground and low-lying excited states for $N \le 5$ can be expressed as $(0,0)^N(\Sigma_I w_I[\Pi_{i=1}^N \exp(-im_i^I\phi_i)/(2\pi)^{1/2}])$. The FCI space comprises all possible configurations with $|m| \le m_{max}$. The size of the one-particle basis set is $2m_{max} + 1$. As show in Table 1, the previous basis set is clearly out-performed by this new representation: the total energies are lowered by using much smaller FCI spaces. For example, the number of FCI configurations is 135 million (30.000) for the previous (new) basis and $N = 4$.

Considering the particular case of two pH_2 molecules, the total wave function at different Λ values can be written as $\sim(0,0)^2 \exp(i\Lambda\phi_+)/(2\pi)^{1/2} f_m^{P_\phi}(\phi_-)$. It contains an azimuthal term depending on the half sum of the azimuthal angles, $\phi_+ = (\phi_1 + \phi_2)/2$ describing the overall rotation around the dopant axis and a term depending on the half difference between the azimuthal angles of the two particles, $\phi_- = \phi_1 - \phi_2$, with m labeling the level and $P_\phi = \pm$ denoting the symmetry with respect to ϕ_- inversion. The wave function part depending on ϕ_- thus describes the pH_2-pH_2 bending motion on the belt. Similarly to studies by Villarreal et al.[20] and Hernández et al.[21] for ^{4}He and $N = 2$, this structure is understood by turning to a reduced

dx.doi.org/10.1021/jz200801r | J. Phys. Chem. Lett. 2011, 2, 2145–2151

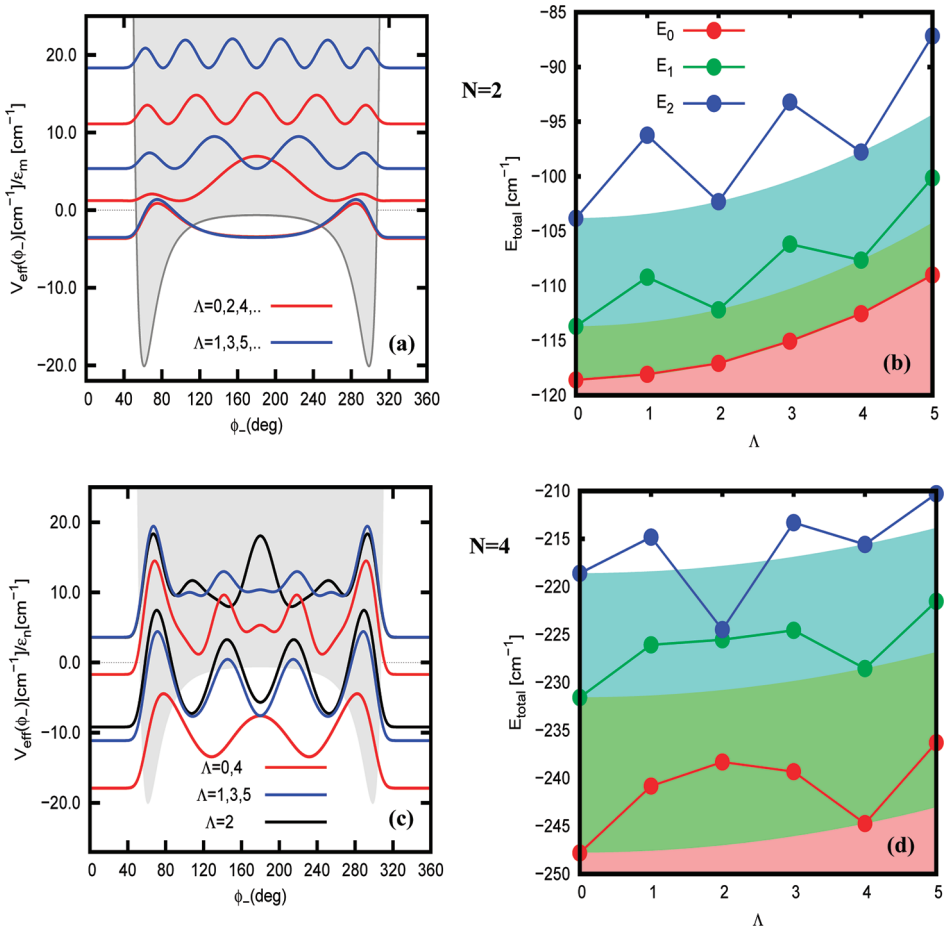

Figure 2. Upper panels: (a) pair density distributions of the $f_m(\phi_-)$ eigenstates (see text) and associated eigenvalues ε_m; (b) total energies of the lowest-energy bands of a $(pH_2)_2{-}CO_2$ cluster. The shaded areas drawn represent the double-well $pH_2{-}pH_2$ potential $V_{eff}(\phi_-)$ (second term on the right side of eq 2). Lower panels: (c) energy levels ε_n (third term on the right side of eq 4) and angular pair density distributions associated to the six lowest-energy bending $pH_2{-}pH_2$ states in a $(pH_2)_4{-}CO_2$ cluster; (d) Total energies of the three lowest-energy bands. The borders between the shaded areas drawn in the right panels indicate that the envelope of the total energy is a quadratic function of Λ. (See the text.)

dimensional model for ϕ_+ and ϕ_- and averaging over the lowest state for the faster r and θ modes

$$\langle H\rangle_{(0,0)} = \left\langle -\frac{\hbar^2}{4\mu r^2}\right\rangle_{(0,0)}\left[\frac{\partial^2}{\partial^2\phi_+} + 4\frac{\partial^2}{\partial^2\phi_-}\right] + \langle V^{pH_2-pH_2}(\phi_-)\rangle_{(0,0)} \quad (2)$$

The term depending on ϕ_+ describes the overall rotation around the dopant axis with a frequency $\sim B^{\parallel}_{eff}/2$. This can be generalized to any number of particles: the wave function dependence on $\phi_+ = (\phi_1 + ... + \phi_N)/N$ can be factorized out as $\exp(i\Lambda\phi_+)/(2\pi)^{1/2}$, giving the contribution to the total energy of $B^{\parallel}_{eff}/N \times \Lambda^2$.

For $N = 2$, as shown in Figure 2a, the eigenvectors associated with the internal mode ϕ_-, owing to the well of the pair interaction, mimic particle-in-a-double-well-like states in contrast with the particle-in-a-box-like states for the less-attractive ^4He case.[20,21] (See also Figure 3d.) We stress here that the position of the energy levels depicted in Figure 2a is nearly coincident with those reported in ref 24 (Figure 5) for the $(pH_2)_2{-}CO_2$ trimer, confirming the accuracy of the adopted approaches. Because a bosonic wave function must be symmetric, $f^+_m(\phi_-)/f^-_m(\phi_-)$ can only be associated with even/odd Λ values.

The wave function part depending on the internal mode is thus repeated with a periodicity of $\Lambda = \Lambda + 2$. More generally, it is clear that the total wave function must kept unaltered when any pH_2 molecule is brought back to the same position on the belt by a rotation with $\phi = 2\pi$. By writing the total wave function as

$$\Psi^{\Lambda}_{(0,0),m}(\{R_i,\theta_i\},\phi_+,\{\phi_i-\phi_j\}) = (0,0)^N(\exp(i\Lambda(\phi_1+...\phi_N)/N)/\sqrt{2\pi})\Phi^m_{int}(\{\phi_i-\phi_j\}) \quad (3)$$

it is easy to show that the internal part of the wave function, $\Phi^m_{int}(\{\phi_i - \phi_j\})$, acquires the phase factor of $\exp(-i\Lambda 2\pi/N)$ when any of relative angles $\phi_i - \phi_j$ changes by 2π. Therefore, the internal eigenvector $\Phi^m_{int}(\{\phi_i - \phi_j\})$ for a given Λ also will be an eigenvector for $\Lambda + \nu N$ for any integer ν. Writing the total energy as

$$E_{total}(\Lambda) = N \times e_0 + \frac{B^{\parallel}_{eff}}{N} \times \Lambda^2 + \varepsilon_n(\Lambda) \quad (4)$$

with e_0 being the energy of the (0,0) orbital, it turns out that the energy arising from the internal motion ε_n is an even periodic

dx.doi.org/10.1021/jz200801r | J. Phys. Chem. Lett. 2011, 2, 2145–2151

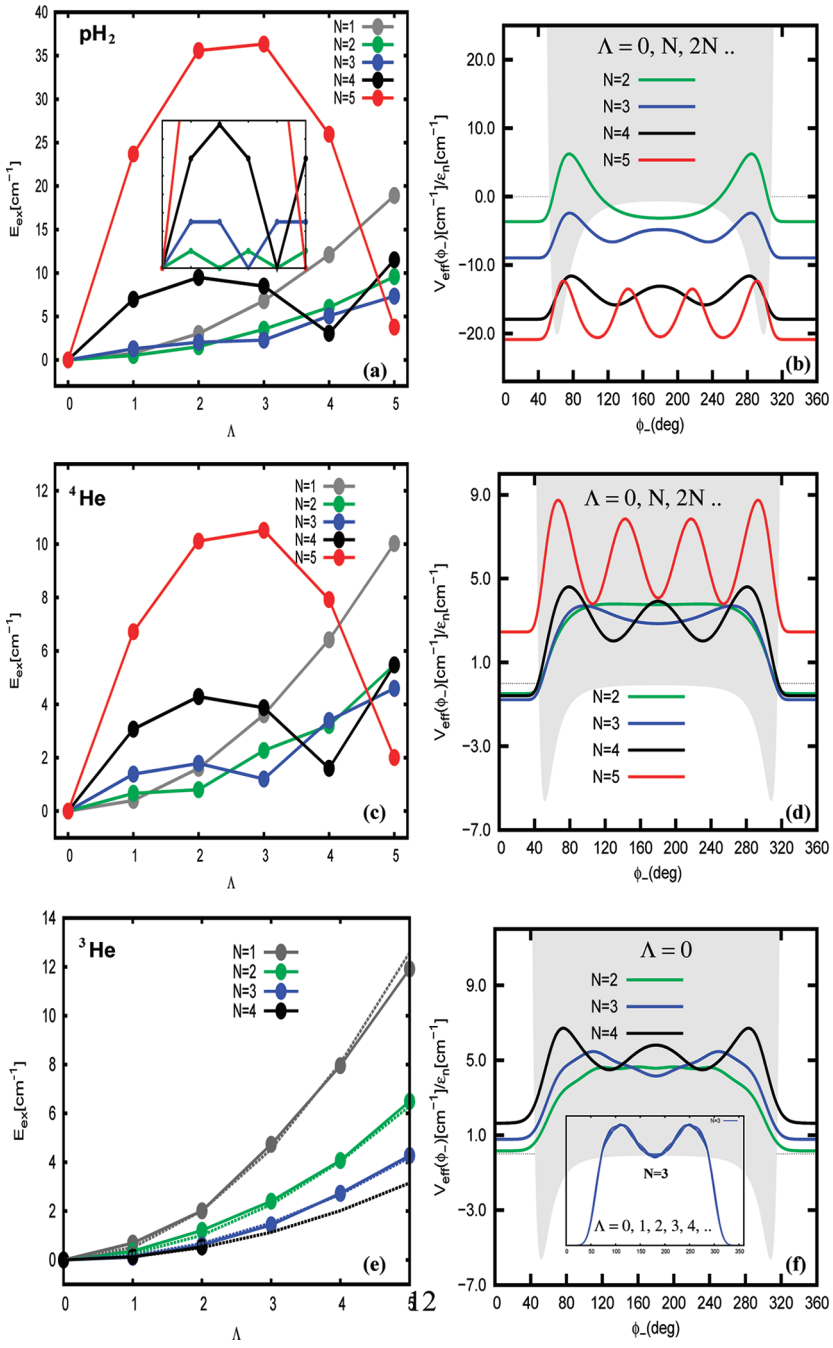

Figure 3. Left panels: (a) excitation energy spectrum of $(pH_2)_N$-CO_2 clusters with an inset showing the periodicity after subtracting the term $B_{eff}^{\|}/N \times \Lambda^2$; (c) the same for $(^4He)_N$-CO_2 clusters; (e) the same for $(^3He)_N$-CO_2 clusters where the dashed lines correspond to the term $B_{eff}^{\|}/N \times \Lambda^2$. Right panels: energy levels ε_n (third term on the right side of eq 4) and pair density distributions of the lowest bending pH_2-pH_2 state for $(pH_2)_N-CO_2$ (b), $(^4He)_N-CO_2$ (d), and $(^3He)_N-CO_2$ clusters and $\Lambda = 0$. (The inset also shown the pair densities for larger Λ values and $N = 3$.) The shaded areas drawn represent the double-well pH_2-pH_2 potential $V_{eff}(\phi_-)$ (second term at the right side of eq 2).

function of Λ. In particular, $\varepsilon_n(\Lambda + N) = \varepsilon_n(\Lambda)$ and $\varepsilon_n(\Lambda - N) = \varepsilon_n(\Lambda)$. As apparent from Figure 2b, the energy spectrum as a function of Λ thus consists of a periodic part having a band-like structure and an envelope that is a quadratic function resulting from the overall rotation. Therefore, by considering that all bosons occupy the (0,0) orbital and removing the overall rotation $B_{eff}^{\|}\Lambda^2/N$ term, the equation for the wave function is strongly reminiscent of that of a N-term polymer with periodic boundary conditions, frequently used to model 1-D periodic solids. The value Λ/N plays the same role as the index k in solid-state theory and in the limit $N \rightarrow \infty$ becomes continuous. Consequently, the energy dependence $\varepsilon_n(\Lambda)$ is the typical one found for solid band-like structures. This was first predicted by Bloch for a system of noninteracting bosons,[28] and we reveal a similar picture. However, it must be stressed that this analogy is only valid within the (0,0) approximation. For cluster sizes for which the second belt starts to be filled, the energy dependence on Λ will deviate from this simple band-like structure. The detailed

dx.doi.org/10.1021/jz200801r |J. Phys. Chem. Lett. 2011, 2, 2145–2151

analysis of this behavior will be presented elsewhere. For $N = 2$, because the two lowest double-well states are quasi-degenerate, the Λ dependence for the lowest-energy band is quasi-quadratic, whereas higher energy bands exhibit a sawtooth-like structure. In addition to the minimum at $\Lambda = 0$ for the nodeless ground-state, the lowest-energy band for $N = 4$ (Figure 2d) also has a minimum at $\Lambda = 4$, whereas second and third bands become entangled at $N/2$. As can be seen in the upper-left panel of Figure 3, the minimum at $\Lambda = N$ becomes more pronounced for $N = 5$.

The fact that for bosons the minimum of ε_0 always corresponds to $\Lambda = 0$ can be understood in a somewhat simplified way, as being due to $\Lambda = 0$ being the only solution allowing for all $m_i = 0$ and so minimizing the kinetic energy. Because of the Fermi principle, this is not possible for fermionic systems, and this is in fact what we have found here (see below). Starting with the zero-order wave function for $\Lambda = 0$ with all $m_i = 0$, the periodic condition implies a solution with all $m_i = \nu$ for states with $\Lambda = \nu N$. Altogether, the existence of energy minima when Λ is an integer multiple of N implies that the excited pH_2 molecules rotate collectively, keeping their relative positions unaltered. The value of $\Lambda = \Sigma_i^N m_i$ is closely related to the azimuthal probability current, $J_\phi(r,\theta) = (\nu/\mu)\rho(r,\theta)$, where $\rho(r,\theta) = N(0,0)^2$ is the one-particle density. As shown in Figure 3b, the ^{4}He clusters have similar behavior, and the band-like structure already exhibits the minimum at $\Lambda = N = 3$. The He-dopant potential was taken from ref 29. The function connecting collective rotational states at $\Lambda = N$ scales as $NB_{\mathrm{eff}}^{\parallel} \times \nu^2$ for any integer ν. It is noticeable that the existence of these "singularities" for bosons on a ring was already connected to the onset of superfluidity by Bloch.[28] Their presence can be anticipated from the energy difference between the lowest-energy and the first-excited bending states (referred to as $\Delta\varepsilon$) because $\varepsilon_0(\Lambda)$ close to $\Lambda = 0$ should rise more rapidly than the term $B_{\mathrm{eff}}^{\parallel}/N \times \Lambda^2$, $2\nu < \Delta\varepsilon/B_{\mathrm{eff}}^{\parallel}$. The magnitude $\Delta\varepsilon$ can be identified with the frequency of the boson−boson bending mode. For pH_2 (^{4}He), the values $\Delta\varepsilon/B_{\mathrm{eff}}^{\parallel}$ at $N = 2$, 3, 4, and 5 are 0.2, 1.4, 9.0, and 30.0 (1.2, 3.0, 7.4 and 16.5). Considering pH_2 with OCS as the dopant, the values are very similar (0.6, 1.5, 8.6, and 30.0). Hence, the possible presence of minima at $N = 2$ and 3 ($N = 2$) for pH_2 (^{4}He) is already ruled out. The frequency of the boson−boson bending mode thus rises steeply at the maximum number of particles on the belt owing to the intensified hard-core repulsion. Because the hard-core of the pH_2−pH_2 potential is more pronounced than in the ^{4}He case, the value $\Delta\varepsilon/B_{\mathrm{eff}}^{\parallel}$ at $N = 5$ is about two times larger for pH_2.

Author: We have extended our calculations to fermionic $(^3\mathrm{He})_N$−CO_2 clusters ($N \leq 4$) by using the basis set comprising spherical harmonics. The lowest left-hand panel of Figure 3 clearly shows that the picture changes completely: regardless of the number of ^{3}He atoms, the lowest energy values as a function of Λ exhibit the normal quasi-quadratic dependence that results from the term $B_{\mathrm{eff}}^{\parallel}/N \times \Lambda^2$. (Also see refs 16 and 17.) In this case, the total wave function for two ^{3}He atoms can be expressed as

$$\Psi^{\Lambda,S,\Sigma}_{(0,0),m}(\{R_i,\theta_i\},\phi_+,\{\phi_i-\phi_j\},\{\sigma_i\}) = (0,0)^2\frac{e^{i\Lambda\phi_+}}{\sqrt{2\pi}}f_m^{P_\phi}(\phi_-)\Xi_{S\Sigma}(\{\sigma_i\}) \quad (5)$$

where σ_i are the spin coordinates of the ^{3}He atoms with total spin angular momentum S and Σ is the S projection on the dopant axis. Altogether, the presence of the spin factor makes the energy associated with the relative motion apparently independent of Λ. This is reflected in the pair densities for $N = 3$; see the inset of Figure 3f, where nearly coincident distributions are obtained whatever the Λ value may be. For $N = 2$, the spin functions are separable from the spatial-only part and are symmetric (singlet) or antisymmetric (triplet) under the exchange of two ^{3}He atoms. Therefore, the lowest-energy (symmetric) bending He−He state associates with either odd or even Λ values by combination with singlet or triplet spin-functions, which thus alternate as a function of Λ. As suggested by Bloch,[28] however, a pairing of the fermionic ^{3}He atoms to stabilize the overall rotational states at $\Lambda = \nu N/2$ is not ruled out. The structural pairing of four ^{3}He atoms around a dopant Cl_2 molecule was already found in ref 15. Further methodological development (in progress) is necessary to clarify this point for larger fermionic clusters. Another interesting issue is how the periodicity condition is modified for bosons with nuclear spin I not equal to zero (e.g., *ortho*-D_2 molecule which is a mixture of $I = 0$ and 2 states).

In summary, when the belt encircling a molecular CO_2 dopant has been populated by at least four pH_2 molecules or three ^{4}He atoms, the excitation spectra as a function of Λ reveal minima at integer multiplets of N, which indicates the stabilization of collective rotational states of the spin-less bosonic species. As a result, the effective rotational constant for the axial rotation increases linearly with N. In contrast, the excitation spectra of the fermionic ^{3}He counterpart retain the quadratic dependence on Λ, which arises from the overall axial rotation. Bosonic symmetry per se is not a sufficient condition, and it is also required that the frequency of the boson−boson bending mode rises up to a critical value that is reached near the completion of the belt in the pH_2 case. In turn, this is due to the intensification of the effective hard-core repulsion and, ultimately, to the fact that bosonic systems composed of either pH_2 or ^{4}He are strongly correlated.

The stabilization of collective rotational states ($\Lambda = 0, N, 2N, \ldots$) at N_c and $N_c - 1$, where N_c is the number of pH_2 molecules completing the first belt, can be correlated with the simultaneous disappearance of the Q branch in the infrared spectrum of linear molecules.[10] In contrast with previous interpretations, however, we found it unnecessary to explain the spectral anomalies in terms of the evidenced high axial symmetry of the pH_2 molecules around the dopant at completion of the belt. As shown in ref 30, absorption selection rules lead to the missing Q branch when only $\Lambda = 0$ states are effectively populated. The possible contribution from levels with $\Lambda = N, 2N, \ldots$ implies a non-negligible population of cluster states with $J = \Lambda$, which is improbable at the low temperatures of the experimental measurements (0.15 or 0.37 K). This is in line with DMC and PIMC results by Whaley and collaborators,[25,26] who numerically demonstrated the superfluidity response around the OCS axis. In fact, there is a clear correlation between the reduction of the quantum moment of inertia on the dopant axis[25] and the increased effective rotational constant for the axial motion with N_c pH_2 molecules. Work is in progress to extend our approach to larger cluster sizes, for which adjacent belts around the molecular dopant become populated. One interesting issue would be to analyze if there is a microscopic mechanism that preserves collective rotational motion on individual belts, making connections with the demonstrated experimentally and estimated theoretically superfluidity response on the direction perpendicular to the dopant axis for larger cluster sizes.[11]

■ ASSOCIATED CONTENT

Ⓢ Supporting Information. Information on total energies of ground and excited states of $(pH_2)_N$−OCS ($N = 2$−5)

clusters by using the pH_2−OCS potential energy surface from ref 31. This material is available free of charge via the Internet at http://pubs.acs.org.

AUTHOR INFORMATION

Corresponding Author

*E-mail: Pilar.deLara.Castells@csic.es.

Notes

[§]E-mail: Alexander.Mitrushchenkov@univ-paris-est.fr.

ACKNOWLEDGMENT

We thank C. Cabrillo, P. Villarreal, M. I. Hernández, N. Halberstadt, J. Navarro, M. Barranco, and A. Salam for stimulating discussions, N. F. Aguirre for his assistance in the abstract graphics, and F. Paesani for kindly providing the pH_2−OCS potential energy surface. This work has been partially supported by the CSIC-CM, DGICYT, and MICINN-CSIC Spanish grant nos. CCG08-CSIC/ESP-3680, FIS2010-18132, and 2007501004. The support of COST Action CM1002 (CODECS) and the program CONSOLIDER-INGENIO 2010 under grant CSD2009-00038 is also acknowledged. The calculations were performed at the Centro de Supercomputación de Galicia (CESGA).

REFERENCES

(1) Toennies, J. P.; Vilesov, A. F. Superfluid Helium Droplets: A Uniquely Cold Matrix for Molecules and Molecular Complexes. *Angew. Chem., Int. Ed.* **2004**, *43*, 2622−2648.

(2) Sindzingre, P.; Ceperley, D. M.; Klein, M. L. Superfluid in Clusters of p−H_2 Molecules. *Phys. Rev. Lett.* **1991**, *67*, 1871−1874.

(3) Tejeda, G.; Fernández, J. M.; Montero, S.; Blume, D.; Toennies, J. P. Raman Spectroscopy of Small Para−H_2 Clusters Formed in Cryogenic Free Jets. *Phys. Rev. Lett.* **2004**, *92*, 223401-1−223401-4.

(4) Navarro, J.; Ancilotto, F.; Barranco, M.; Pi, M. Towards a Density Functional Description of Liquid pH_2. *J. Phys. Chem. A* **2011**, *115*, 6910−6717.

(5) Kim, E.; Chan, M. H. W. Probable Observation of a Supersolid Helium Phase. *Nature (London)* **2004**, *427*, 225−227.

(6) Pratt, E. J.; Hunt, B.; Gadagkar, V.; Yamashita, M.; Graf, M. J.; Balatsky, A. V.; Davis, J. C. Interplay of Rotational, Relaxational, and Shear Dynamics in Solid ^{4}He. *Science* **2011**, *332*, 821−824.

(7) Kwon, Y.; Whaley, K. B. Nanoscale Molecular Superfluidity of Hydrogen. *Phys. Rev. Lett.* **2002**, *89*, 273401-1−273401-4.

(8) Paesani, F.; Zillich, R. E.; Known, Y.; Whaley, K. B. OCS in *para*-Hydrogen Clusters: Rotational Dynamics and Superfluidity. *J. Chem. Phys.* **2005**, *122*, 181106-1−181106-4.

(9) Grebenev, S.; Sartakov, B.; Toennies, J. P.; Vilesov, A. F. Spectroscopic Investigation of OCS−$(p$-$H_2)_n$ (n = 1−16) Complexes Inside Helium Droplets: Evidence for Superfluid Behavior. *J. Chem. Phys.* **2010**, *132*, 064501-1−064501-19.

(10) Grebenev, S.; Sartakov, B.; Toennies, J. P.; Vilesov, A. F. Evidence for Superfluidity in *para*-Hydrogen Clusters Inside Helium-4 Droplets at 0.15 K. *Science* **2000**, *289*, 1532−1535.

(11) Li, H.; Le Roy, R. J.; Roy, P. N.; McKellar, A. Molecular Superfluid: Nonclassical Rotations in Doped *para*-Hydrogen Clusters. *Phys. Rev. Lett.* **2010**, *105*, 133401-1−133401-4.

(12) Baroni, S.; Moroni, S. In *Quantum Monte Carlo Methods in Physics and Chemistry*; Nightingale, P., Umrigar, C. J., Eds.; NATO Series 525, Kluwer Academic: Boston, 1999.

(13) de Lara-Castells, M. P.; Delgado-Barrio, G.; Villarreal, P.; Mitrushchenkov, A. O. A Full-Configuration Interaction Nuclear Orbital Method to Study Doped ^3He_N Clusters. *J. Chem. Phys.* **2006**, *125*, 221101-1−221101-4.

(14) de Lara-Castells, M. P.; Mitrushchenkov, A. O.; Delgado-Barrio, G.; Villarreal, P. Using a Jacobi-Davidson Nuclear Orbital Method for Small Doped ^{3}He Clsuters. *Few-Body Syst.* **2009**, *45*, 233−236.

(15) de Lara-Castells, M. P.; Delgado-Barrio, G.; Villarreal, P.; Mitrushchenkov, A. O. An Optimized Full-Configuration-Interaction Nuclear Orbital Approach to a Hard-Core Interaction Problem: Application to (^3He_N)−$Cl_2(B)$ clusters ($N \leq 4$). *J. Chem. Phys.* **2009**, *131*, 194101-1−194101-13.

(16) de Lara-Castells, M. P.; Aguirre, N. F.; Villarreal, P.; Delgado-Barrio, G.; Mitrushchenkov, A. O. Quantum Solvent States and Rovibrational Spectra of Small Doped ^{3}He Clusters Through the Full-Configuration Interaction Nuclear Orbital Approach. *J. Chem. Phys.* **2010**, *132*, 194313-1−194313-14.

(17) de Lara-Castells, M. P.; Villarreal, P.; Delgado-Barrio, G.; Mitrushchenkov, A. O. Microscopic Description of Small Doped ^{3}He Clusters Through the Full-Configuration Interaction Nuclear Orbital Approach: The $(^3He)^N$-$Br_2(X)$ Case Revisited. *Int. J. Quantum Chem.* **2011**, *111*, 406−415.

(18) Jungwirth, P.; Krylov, A. I. Small Doped ^{3}He Clusters: A Systematic Quantum Chemistry Approach to Fermionic Nuclear Wave Functions and Energies. *J. Chem. Phys.* **2001**, *115*, 10214−10219.

(19) de Lara-Castells, M. P.; López-Durán, D.; Delgado-Barrio, G.; Villarreal, P.; Di Paola, C.; Gianturco, F. A.; Jellinek, J. Energies and Density Distributions of $(^4He)_N$ Clusters Doped with Br_2: A Hartree-Like Approach. *Phys. Rev. A* **2005**, *71*, 033203.

(20) Villarreal, P.; Roncero, O.; Delgado-Barrio, G. Energy Levels and Structure of Tetra-Atomic van der Waals Clusters. *J. Chem. Phys.* **1994**, *101*, 2217−2230.

(21) Hernández, M. I.; Halberstadt, N.; Sands, W. D.; Janda, K. C. Structure and Spectroscopy of the He_2−Cl_2 van der Waals Cluster. *J. Chem. Phys.* **2000**, *113*, 7252−7267.

(22) Felker, P. M. Solvent Configuration-Interaction Calculations of Intermolecular States in Molecule-$(Atom)_N$ Clusters: Application to Br_2-^4He_N. *J. Chem. Phys.* **2006**, *125*, 184313−(1−12).

(23) Li, H.; Roy, P. N.; Le Roy, R. J. An Adiabatic-Hindered-Rotor Treatment Allows *para*-H_2 to be Treated As if It Were Spherical. *J. Chem. Phys.* **2010**, *133*, 104305-1−104305-9.

(24) Li, H.; McKellar, A.; Le Roy, R. J.; Roy, P. N. Theoretical and Experimental Study of Weakly Bound CO_2−$(pH_2)_2$ Trimers. *J. Phys. Chem. A* **2011**, *115*, 7327−7337.

(25) Kwon, Y.; Whaley, K. B. Superfluid Response in $OCS(H_2)_5$ and $OCS(D_2)_5$. *J. Low Temp. Phys.* **2005**, *140*, 227−240.

(26) Paesani, F.; Zillich, R. E.; Whaley, K. B. OCS in Small Para-Hydrogen Clusters: Energetics and Structure with N = 18 Complexed Hydrogen Molecules. *J. Chem. Phys.* **2003**, *119*, 11682−11694.

(27) Piccarreta, C.; Gianturco, F. A. The Structuring of a Molecular Dopant in a Quantum Solvent OCS−$(H_2)_N$ van der Waals Clusters. *Eur. Phys. J. D* **2006**, *37*, 93−103.

(28) Bloch, F. Superfluidity in a Ring. *Phys. Rev. A* **1973**, *7*, 2187−2191.

(29) Li, H.; Blinov, N.; Roy, P. N.; Le Roy, R. J. Path-Integral Monte Carlo Simulation of ν_3 Vibrational Shifts for CO_2 in $(He)_N$ Clusters Critically Tests the $HeCO_2$ Potential Energy Surface. *J. Chem. Phys.* **2009**, *130*, 144305-1−144305-11.

(30) de Lara-Castells, M. P.; Prosmiti, R.; López-Durán, D.; Delgado-Barrio, G.; Villarreal, P.; Di Paola, C.; Gianturco, F. A.; Jellinek, J. Polar Di-Halogen Molecules Solvated in Bosonic Helium Clusters: The Paradigm of ICl (X). *Phys. Rev. A* **2006**, *74*, 053201-1−053201-11.

(31) Paesani, F.; Whaley, K. B. Potential Energy Surface and Infrared Spectra of OCS-Hydrogen Complexes. *Mol. Phys.* **2006**, *104*, 61−72.